Overexpression of Insulin-like Growth Factor-1 in Mice Protects from Myocyte Death after Infarction, Attenuating Ventricular Dilation, Wall Stress, and Cardiac Hypertrophy

Qiong Li,* Baosheng Li,* Xiaowei Wang,* Annarosa Leri,* Kumar P. Jana,* Yu Liu,* Jan Kajstura,* Renato Baserga,‡ and Piero Anversa*

**Department of Medicine, New York Medical College, Valhalla, New York 10595; and ‡Kimmel Cancer Center, Thomas Jefferson University, Philadelphia, Pennsylvania 19107*

Abstract

To determine whether IGF-1 opposes the stimulation of myocyte death in the surviving myocardium after infarction, transgenic mice overexpressing human IGF-1B in myocytes (FVB.Igf+/−) and wild-type littermates at 1.5 and 2.5 mo of age were subjected to coronary ligation and killed 7 d later. Myocardial infarction involved an average 50% of the left ventricle, and produced cardiac failure. In the region proximate to infarction, myocyte apoptosis increased 4.2-fold and 2.1-fold in nontransgenics at 1.5 and 2.5 mo, respectively. Corresponding increases in myocyte necrosis were 1.8-fold and 1.6-fold. In contrast, apoptotic and necrotic myocyte death did not increase in FVB.Igf+/− mice at either age after infarction. In 2.5-mo-old infarcted nontransgenics, functional impairment was associated with a 29% decrease in wall thickness, 43% increase in chamber diameter, and a 131% expansion in chamber volume. Conversely, the changes in wall thickness, chamber diameter, and cavitary volume were 41, 58, and 48% smaller in infarcted FVB.Igf+/− than in nontransgenics. The differential response to infarction of FVB.Igf+/− mice resulted in an attenuated increase in diastolic wall stress, cardiac weight, and left and right ventricular weight-to-body wt ratios. In conclusion, constitutive overexpression of IGF-1 prevented activation of cell death in the viable myocardium after infarction, limiting ventricular dilation, myocardial loading, and cardiac hypertrophy. (*J. Clin. Invest.* 1997. 100:1991–1999.) Key words: IGF-1 in myocytes • apoptotic and necrotic myocyte cell death • heart failure • myocardial loading • ventricular remodeling

Introduction

Ventricular dilation acutely after infarction is characterized by depressed cardiac performance, poor recovery of function, and increased mortality (1). The expansion in cavitary volume shortly after coronary artery occlusion is due to an architectural rearrangement of myocytes in the surviving portion of the ventricle, resulting in mural thinning and an increase in the transverse and longitudinal chamber diameters (2–5). Conversely, the infarcted region of the wall contributes minimally to the acute augmentation in diastolic volume of the injured ventricle (6). The underlying mechanism responsible for wall restructuring, side-to-side slippage of cells, and cardiac dilatation has been linked to programmed myocyte death (6, 7). Apoptosis occurs in a scattered manner throughout the nonischemic myocardium, and it affects the border zone more than the remote healthy tissue (7). Physical forces coupled with diastolic Laplace overloading after infarction may play a critical role in the initiation of the endogenous cell death pathway, a possibility that is consistent with recent observations in vitro (8). Since IGF-1 interferes with activation of apoptosis in several cells and organ systems (9–17), the hypothesis was advanced that transgenics overexpressing IGF-1 in myocytes may sustain more effectively the impact of infarction by attenuating cell death stimulation in the spared myocardium. This protective effect may limit cavitary dilation and mural thinning, reducing the overload on the infarcted heart. For this purpose, coronary artery ligation was performed in heterozygous transgenic mice, designated as FVB.Igf+/−, in which the cDNA for the human IGF-1B was placed under the control of the rat α-myosin heavy chain promoter (18). Two age intervals were examined. In comparison with nontransgenics, FVB.Igf+/− mice at 1.5 mo have the same heart weight and 21% more myocytes of smaller size. At 2.5 mo of age, FVB.Igf+/− have hypertrophied hearts and a 31% higher number of cells of similar volume than in nontransgenics (18). These conditions allowed us to discern whether the ability of IGF-1 to oppose cell death after infarction was influenced by cardiac weight or by the volume and number of myocytes.

Methods

Myocardial infarction. Experiments included transgenic FVB.Igf+/− mice and nontransgenic littermates that were developed in our laboratory (18). Under ether anesthesia, the thorax was opened, the heart was exteriorized, and the left main coronary artery was ligated. The chest was then closed, the pneumothorax was reduced, and the animals were allowed to recover. Control mice underwent sham operation. Coronary occlusion was performed in 10 and 38 FVB.Igf+/− at 1.5 and 2.5 mo of age, and mortality affected 5 and 18 animals in the younger and older groups, respectively. The remaining 5 and 20 mice were killed 7 d later. 12 and 42 nontransgenics at 1.5 and 2.5 mo, were subjected to coronary occlusion. 7 in the first group and 22 in the second died during the 7-d period of experimentation. The 5 and 20 surviving mice were included in the study. Sham-operated FVB.Igf+/− and nontransgenics consisted of 5 and 18 animals each at 1.5 and 2.5 mo of age. All mice were injected intraperitoneally with 10 μg of monoclonal antibody specific for cardiac myosin (clone CCM-52) 24 h before death (19, 20).

Address correspondence to Piero Anversa, M.D., Department of Medicine, Vosburgh Pavillion-Room 302, New York Medical College, Valhalla, New York 10595. Phone: 914-594-4168; FAX: 914-594-4406.

Received for publication 18 April 1997 and accepted in revised form 20 August 1997.

J. Clin. Invest.

0021-9738/97/10/1991/09 $2.00
Volume 100, Number 8, October 1997, 1991–1999
http://www.jci.org

Cardiac function. Physiologic measurements were obtained in FVB.Igf+/− and nontransgenic littermates at 2.5 mo of age. Under intraperitoneal chloral hydrate anesthesia, 400 mg/kg body weight, the right carotid artery was cannulated with a microtip pressure transducer catheter (SPR-612; Millar Instruments Inc., Houston, TX) connected to an electrostatic chart recorder (ES 2000; Gould Inc., Cleveland, OH). The catheter was advanced into the left ventricle for evaluation of left ventricular pressures and + and − dP/dt in the closed-chest preparation.

Terminal deoxynucleotidyl transferase (TdT)[1] and myosin antibody labeling. After the hemodynamic measurements, the heart was arrested in diastole (6), and the left ventricle inclusive of the septum and right ventricle were dissected and weighed. Three sections from each left ventricle, cut perpendicularly to the major axis of the heart, were sampled, and frozen sections were obtained. These sections were incubated with TRITC-labeled anti–mouse IgG, fixed in 1.5% paraformaldehyde, and mounted. TdT assay was performed by incubating sections with 5 U of TdT, 2.5% mM $CoCl_2$, 0.2 M potassium cacodylate, 25 mM Tris-HCl, 0.25% BSA, and 0.5 nM biotinylated 2′ deoxyuridine-5′-triphosphate (biotin-16-dUTP). After exposure to 5 μg/ml of FITC-labeled Extravidin, myocytes were stained with α-sarcomeric actin antibody (clone 5C5; Sigma Chemical Co., St. Louis, MO), and then TRITC-labeled anti–mouse IgG and nuclei were visualized with bisbenzimide (7, 8, 20). Myocardial infarction was determined by measuring the fractional area occupied by healing tissue in each of these sections of each ventricle, and the values were averaged. This part of the study included five animals each of sham-operated infarcted FVB.Igf+/− and nontransgenics at 1.5 and 2.5 mo, for a total of 40 mice.

Quantitative analysis of dUTP and myosin labeling in the myocardium. In noninfarcted mice, these analyses were performed in all three sections of myocardium obtained from the base to the apex of the left ventricle. A similar approach was followed in infarcted mice, although involvement of the left ventricular free wall by infarction restricted quantification to the surviving portion of the wall which was adjacent to the infarcted region and to the interventricular septum. The number of myocyte nuclei labeled by dUTP per unit area of myocardium was measured in each left ventricle by examining a minimum of 5.1 to a maximum of 10.5 mm^2. The numerical density of myocyte nuclei was measured by counting the number of bisbenzimide-labeled nuclei in α-sarcomeric actin–positive cells. These values were used to compute the number of apoptotic myocyte nuclei per 10^6 cells (7, 8, 20, 21). Similarly, the number of myocyte profiles labeled by myosin antibody was assessed and expressed per mm^2 of myocardium in each animal (20, 21). The specificity of the TdT reaction for myocyte apoptosis was determined by confocal microscopy. By this procedure, chromatin alterations were correlated with the presence or absence of dUTP labeling in nuclei (22). Chromatin was visualized by propidium iodide (10 mg/ml), and dUTP and α-sarcomeric actin staining were performed as described above. Sections were examined at 100× (numerical aperture 1.3) with a MRC-1000 confocal microscope (Bio-Rad Laboratories, Richmond, CA) (22). A total of 200 myocyte nuclei were examined by sampling 10 nuclei from each of 20 infarcted mice. These nuclei were collected from the basal and midmyocardial regions in each left ventricle.

DNA gel electrophoresis. To confirm that histochemical detection of DNA fragments reflected internucleosomal DNA cleavage, low molecular weight DNA was extracted from isolated ventricular myocytes and analyzed by agarose gel electrophoresis (7, 8). Myocytes were isolated from 2.5-mo-old animals by collagenase perfusion according to a procedure repeatedly used in our laboratory (7, 18, 20). Consistent with previous results, the degree of contamination from nonmyocytes ranged from 1–3%. This part of the study included three and five animals each from sham-operated and infarcted FVB.Igf+/− and nontransgenic littermates, for a total of 16 mice. Myocytes from the region bordering the infarct and septum were fixed in ethanol and incubated in 40 μl of phosphate-citrate buffer (pH 7.8). The supernatant was concentrated and digested with RNase, 1 mg/ml, and Proteinase K, 1 mg/ml. Subsequently, 12 μl of loading buffer (0.25% bromophenol blue, 30% glycerol) was added, and samples were subjected to electrophoresis on 2% agarose gel containing 0.5 μg/ml ethidium bromide. The DNA in the gels was visualized under UV light.

Perfusion fixation and ventricular anatomy. In 10 sham-operated and 10 infarcted FVB.Igf+/− at 2.5 mo, and in an identical number of noninfarcted and infarcted nontransgenics, the abdominal aorta was cannulated with a polyethylene catheter and filled with phosphate buffer (0.2 M, pH 7.4) and heparin (100 IU/ml). In rapid succession, the heart was arrested in diastole by injection of 0.15 ml cadmium chloride (100 mM) through the aortic catheter, the thorax was opened, perfusion with phosphate-buffered formalin was started, and the right atrium was cut to allow drainage (6, 23, 24). Perfusion pressure was adjusted to the mean arterial pressure. The left ventricular chamber was filled with fixative from a pressure reservoir set at a height equivalent to the in vivo–measured end-diastolic pressure for a 20-min fixation (24), a task accomplished by inserting a 25G3/4 Vacutainer (Becton Dickinson Co., Rutherford, NJ) into the left ventricle through the apex. At the end of the procedure, the left ventricle including the septum and the right ventricle were dissected and weighed. After measuring the major longitudinal intracavitary diameter, each left ventricle was serial-sectioned into three rings perpendicular to the major axis of the heart, after which the thickness of the free wall and septum and the transverse chamber diameter were measured by an image analyzer. At the midregion, the minimal and maximal luminal diameters were used with the long axis to compute chamber volume (25). Measurements of wall thickness, chamber radius, and end-diastolic pressure were used to calculate wall stress at each of the three sites examined (24, 26). Infarct size in these hearts was determined as described above.

Data collection and analysis. Tissue samples were coded, and the code was broken at the end of the experiments. Results are presented as mean±SD. Statistical significance ($P < 0.05$) between two measurements and among multiple groups was determined by the two-tailed Student's *t* test, ANOVA and the Bonferroni method, respectively (27). Specifically, the changes in the magnitude of myocyte apoptosis and necrosis in each region of the heart in nontransgenic and transgenic mice were established by Student's *t* test (two-group analysis), whereas the baseline difference in the two regions of the heart in the two groups of animals were determined by the Bonferroni method (four-group analysis). Infarct size at the two age intervals in each animal group was compared by Student's *t* test (two-group analysis), but infarct size among the four groups of infarcted mice was evaluated by the Bonferroni method (four-group analysis). Functional measurements between control and infarcted mice in each group were analyzed by Student's *t* test (two-group analysis). A four-group analysis by Bonferroni method, however, was performed when physiologic parameters were compared in noninfarcted and infarcted transgenic and nontransgenic mice. The differences in relative changes of wall thickness, chamber diameter, and chamber volume between infarcted nontransgenic and transgenic animals were computed from the quotient of values of noninfarcted and infarcted animals in each group, according to the equation previously described (28). Subsequently, a Student's *t* test was applied.

Results

Myocyte death. Nuclear damage and TdT labeling of myocytes were apparent by confocal microscopy 7 d after infarction in nontransgenics (Figs. 1, *A–D*). Myocyte necrosis, detected by myosin antibody, was also evident with this tech-

1. *Abbreviations used in this paper:* IGF-1R, IGF-1 receptor; LVEDP, left ventricular end-diastolic pressure; LVSP, left ventricular systolic pressure; MI, effects of infarction; SO, sham-operated; TdT, terminal deoxynucleotidyl transferase.

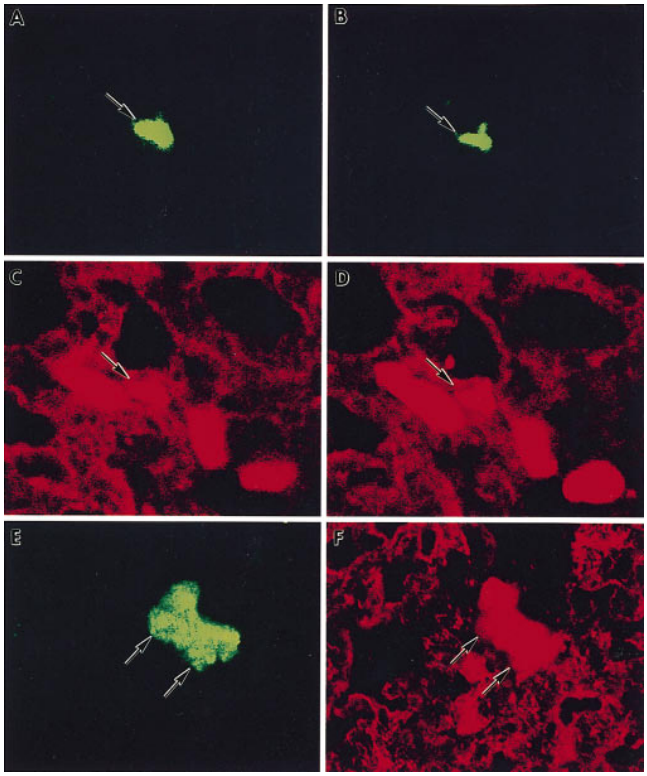

Figure 1. Confocal microscopy of ventricular myocardium of a nontransgenic mouse 7 d after infarction. The same apoptotic nucleus (*arrows*) is illustrated at two optical levels, *A* and *B*, and *C* and *D*. *A* and *B* document by green fluorescence dUTP labeling, and *C* and *D* by red fluorescence propidium iodide staining of nuclei (*arrows*) and α-sarcomeric actin labeling of the myocyte cytoplasm. *B* and *D* demonstrate initial nuclear fragmentation, which was not apparent in *A* and *C*. *A–D*, 1,200×. Myosin antibody labeling of a necrotic myocyte (*arrowheads*) is shown in *E*. α-sarcomeric actin staining of the myocyte cytoplasm is illustrated in *F*. *A–D*, 900×; *E* and *F*, 600×.

nique (Figs. 1, *E* and *F*). The analysis of 200 TdT-positive myocyte nuclei demonstrated that 91±8% showed TdT labeling and chromatin damage, and 9±8% showed positive staining in the absence of nuclear alterations. Since formation of DNA strand breaks precedes changes in chromatin structure (29), the specificity of histochemical detection of apoptosis was confirmed here by confocal microscopy. Low levels of apoptosis were observed in the left ventricle and septum of control nontransgenics and FVB.Igf+/− at 1.5 and 2.5 mo (Fig. 2). Myocardial infarction resulted in a 4.2-fold ($P < 0.001$) and 2.1-fold ($P < 0.002$) increase in myocyte apoptosis in the surviving portion of the left ventricle in nontransgenics at 1.5 and 2.5 mo, respectively. Smaller changes were detected at the level of the septum, but they were not significant. Fig. 2 also shows the effects of myocardial infarction on FVB.Igf+/− mice. In these animals, there was no increase in apoptotic myocyte cell death in the left ventricle and septum at either age. Before coronary ligation, the degree of apoptosis in transgenics at 1.5 and 2.5 mo was consistently lower than in nontransgenics, but these differences were statistically significant only in the left ventricular free wall at the later age interval ($P < 0.01$). Moreover, baseline myocyte apoptosis in the left ventricle was greater than in the septum in FVB.Igf+/− at 1.5 mo ($P < 0.003$) and in nontransgenic mice at 2.5 mo ($P < 0.01$).

Myocyte necrosis was comparable in control transgenic and nontransgenic mice (Fig. 3). In the absence of infarction, myocyte necrosis affected the left ventricle more than the septum in nontransgenics at 1.5 ($P < 0.001$) and 2.5 mo ($P < 0.001$) as well as in transgenics at 1.5 ($P < 0.001$) and 2.5 mo ($P < 0.001$) of age. Coronary ligation increased this form of myocyte death in nontransgenics at 1.5 and 2.5 mo, but had no influence on FVB.Igf+/− at both ages. Similarly to apoptosis, infarction enhanced necrotic cell death in nontransgenics only in the left ventricle. In this region, there was a 1.8-fold ($P < 0.02$) and 1.6-fold ($P < 0.03$) increase at 1.5 and 2.5 mo.

Infarct size was measured in the four groups of animals included in this part of the study and in the section below, describing ventricular anatomy (Fig. 4). In nontransgenic mice at 1.5 and 2.5 mo, infarct size at 7 d was 58±6% ($n = 5$) and 50±6% ($n = 15$), respectively. The 16% higher value in the younger animals was significant ($P < 0.02$). Infarct dimension in transgenic mice was 54±8% ($n = 5$) at 1.5, and 49±5% ($n = 15$) at 2.5 mo, but this 10% difference did not reach statistical significance. Moreover, infarct size was comparable in FVB.Igf+/− and nontransgenic mice at the two age intervals examined.

DNA laddering. To confirm that TdT staining of nuclei corresponded to DNA fragmentation, low molecular weight DNA was extracted from ventricular myocytes of 2.5-mo-old mice and analyzed by agarose gel electrophoresis. Myocytes from control FVB.Igf+/− and nontransgenic mice did not show

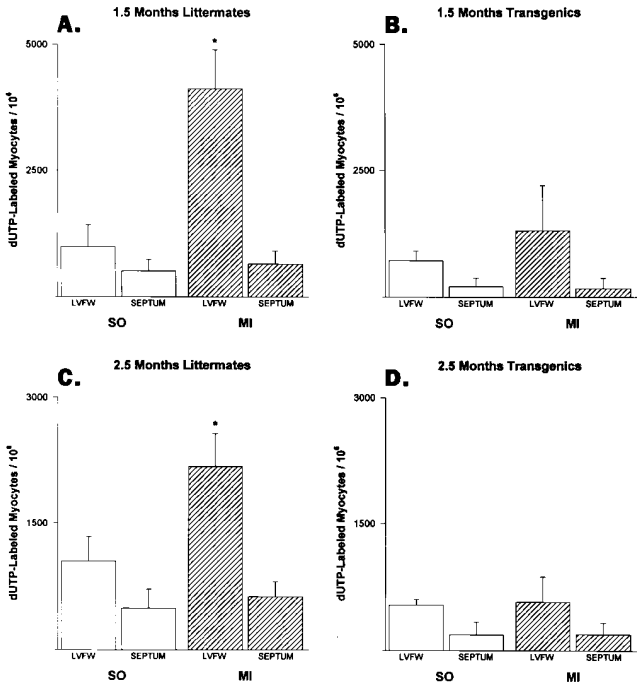

Figure 2. Effects of infarction on apoptosis in the viable left ventricular free wall (*LVFW*) and septum (*septum*) in nontransgenics and transgenics. *Indicates a difference from control mice, $P < 0.05$. Although not indicated for simplicity, apoptosis in the LVFW of control FVB.Igf+/− is higher than in the septum at 1.5 ($P < 0.003$) and 2.5 ($P < 0.002$) mo. A similar difference was noted in control nontransgenics at 2.5 mo ($P < 0.01$). $n = 5$ in each group.

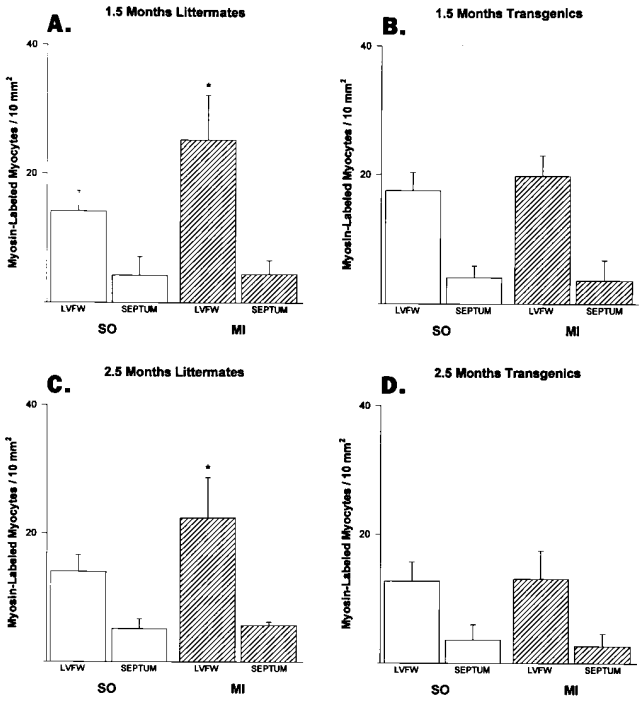

Figure 3. Effects of infarction on necrosis in the viable left ventricular free wall (*LVFW*) and septum (*septum*) in nontransgenics and transgenics. *Indicates a difference from control mice, $P < 0.05$. Although not indicated for simplicity, necrosis in the LVFW of control nontransgenics is higher than in the septum at 1.5 ($P < 0.02$) and 2.5 ($P < 0.001$) mo. Similar differences were noted in control FVB.Igf+/− at 1.5 ($P < 0.001$) and 2.5 ($P < 0.001$) mo. $n = 5$ in each group.

DNA laddering. Conversely, internucleosomal cleavage was apparent in nontransgenics after infarction (Fig. 5, lanes *2* and *3*). DNA damage, however, was not detected in infarcted FVB.Igf+/− mice (Fig. 5, lane *4*).

Ventricular anatomy and wall stress. Heart weight of control nontransgenics (left ventricle [LV] = 103±13 mg; right ventricle [RV] = 34±4 mg; $n = 5$) and transgenics (LV = 115±11 mg; RV = 38±4 mg; $n = 5$) did not differ at 1.5 mo. A 26% ($P < 0.001$) and 41% ($P < 0.001$) greater value, however, was observed in the left and right ventricles of FVB.Igf+/− (LV = 164±9 mg; RV = 62±4 mg; $n = 15$) than in those of nontransgenics (LV = 130±9 mg; RV = 44±3 mg; $n = 15$) at 2.5 mo. In younger nontransgenics, infarction did not change left (108±17 mg; $n = 5$) or right (36±6 mg; $n = 5$) ventricular weights. Body weight also did not vary (from 22.7±3.1 g to 21.5±3.4 g), resulting in similar cardiac weight-to-body weight ratios. In older infarcted nontransgenics, a 23% ($P < 0.001$) increase in the left (160±7 mg; $n = 15$) and a 27% ($P < 0.001$) in the right (56±5 mg; $n = 15$) ventricular weight was found, while body weight decreased 8% ($P < 0.05$) from 25.3±1.4 to 23.4±3.0 g.

In infarcted FVB.Igf+/− at 1.5 mo, the weight of the left (129±16 mg; $n = 5$) and right (43±6 mg; $n = 5$) ventricles remained constant. Body weight was also not affected by infarction (from 24.1±2.8 to 23.6±4.8 g) and cardiac weight-to-body weight ratios did not change. A 15% ($P < 0.001$) and 13% ($P < 0.05$) increase in the weight of the left (189±16 mg; $n = 15$) and right (70±6 mg; $n = 15$) ventricles, however, was observed in infarcted transgenics at 2.5 mo, whereas body weight decreased 6% ($P < 0.05$) from 27±1.7 to 25.5±2.1 g. As a consequence of these alterations in the older animal groups, infarcted nontransgenics at 2.5 mo showed a 35 ($P < 0.001$), 40 ($P < 0.001$), and 36% ($P < 0.001$) increase in the left ventricle (sham-operated [SO] = 5.2±0.2 mg/g; effects of infarction [MI] = 7.0±0.8 mg/g), right ventricle (SO = 1.74±0.06 mg/g; MI = 2.44±0.29 mg/g), and total heart (SO = 6.9±0.3 mg/g; MI = 9.4±1.1 mg/g) weight-to-body weight ratio. Corresponding increases in infarcted FVB.Igf+/− were 21% (SO = 6.1±0.4 mg/g; MI = 7.4±0.4 mg/g, $P < 0.001$), 19% (SO = 2.31±0.16 mg/g; MI = 2.75±0.13 mg/g, $P < 0.001$) and 21% (SO = 8.4±0.6 mg/g; MI = 10.2±0.5 mg/g, $P < 0.001$).

Functional measurements could not be obtained in animals at 1.5 mo because of the small size of the heart. These determinations were restricted to FVB.Igf+/− (control, $n = 18$; infarcted, $n = 20$) and nontransgenics (control, $n = 18$; infarcted, $n = 20$) at 2.5 mo. Left ventricular systolic pressure (LVSP), left ventricular end-diastolic pressure (LVEDP), and left ventricular + and − dP/dt were comparable in control nontransgenic (LVSP = 116±10 mgHg; LVEDP = 10±4 mgHg; +dP/d*t* = 9,038±795 mmHg/s; −dP/d*t* = 7,103±907 mmHg/s) and FVB.Igf+/− mice (LVSP = 108±21 mmHg; LVEDP = 11±3 mmHg; +dP/d*t* = 8,886±1,372 mmHg/s; −dP/d*t* = 7,314±1,359 mmHg/s). Myocardial infarction increased LVEDP (nontransgenic, 27±4 mgHg; FVB.Igf+/−, 24±5 mgHg; $P < 0.001$) and decreased LVSP (nontransgenic, 87±13 mgHg; FVB.Igf+/−, 89±9 mmHg; $P < 0.001$), +dP/dt (nontransgenic, 6,456±1,565 mmHg/s; FVB.Igf+/−, 6,894±1,418 mmHg/s; $P < 0.001$) and −dP/dt (nontransgenic, 5,116 ±1,269

Figure 4. Reconstruction by confocal microscopy of an infarct in a FVB.Igf+/− mouse involving most of the left ventricular free wall. Red fluorescence corresponds to α-sarcomeric actin staining of viable myocytes. Septum, IS; right ventricle, RV. 15×.

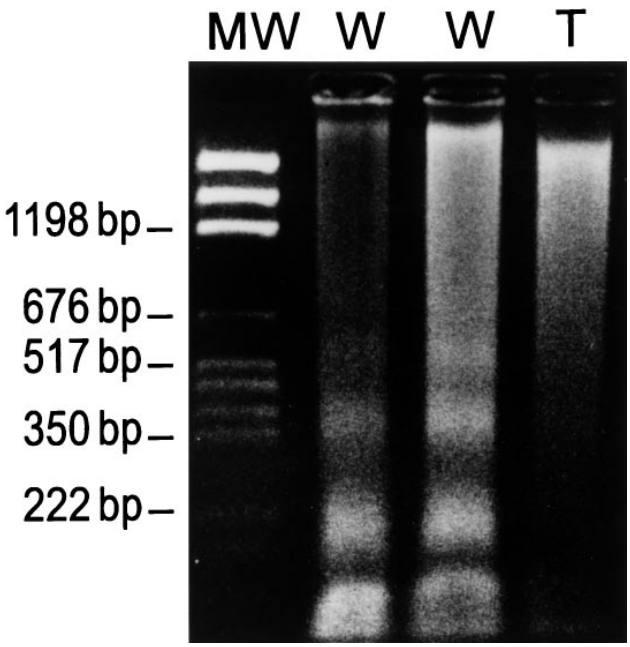

Figure 5. Detection of DNA fragments corresponding to mono and oligonucleosomes in myocytes isolated from the viable left ventricle of infarcted nontransgenics (*W*) and transgenics (*T*). Molecular markers are shown on the left. DNA fragments of nearly 200, 400, and 600 bp are apparent in infarcted nontransgenics.

mmHg/s; FVB.Igf+/−, 5,220±1,258 mmHg/s; $P < 0.001$). Although the changes in LVEDP, LVSP, and dP/dt were greater in nontransgenics, these differences were not significant.

Fig. 6 illustrates the changes in wall thickness and chamber diameter after infarction at each of the three levels of the left ventricle from base to apex in nontransgenics and transgenics. This analysis included 10 mice in each group. In comparison with sham-operated nontransgenics, infarcted animals showed a 24% ($P < 0.005$), 22% ($P < 0.05$), and 42% ($P < 0.001$) decrease in the thickness of the viable portion of the left ventricle, resulting in an average 29% ($P < 0.001$) decrease in this parameter (Fig. 6 *A*). Septal thickness was not altered after infarction (not shown). Conversely, chamber diameter increased 37% ($P < 0.001$), 39% ($P < 0.001$), and 55% ($P < 0.001$) from base to apex, producing a 43% ($P < 0.001$) augmentation in the entire ventricle (Fig. 6 *B*). In FVB.Igf+/− mice, myocardial infarction was characterized by the lack of changes in the thickness of the left ventricle at the base. A 23% ($P < 0.005$) and 31% ($P < 0.001$) reduction, however, was noted in the middle and inferior portions (Fig. 6 *C*), resulting in an average decrease of 17% ($P < 0.01$). Septal thickness remained constant at the three levels (not shown). The regional changes in wall thickness from the base to the apex of the ventricle after infarction in both nontransgenic and transgenic mice were independent from the infarcted myocardium, which was excluded from the measurements. This variability may reflect the complexity of ventricular remodeling in the postinfarcted heart. Chamber diameter increased 21% ($P < 0.05$) and 31% ($P < 0.001$) in the lower two-thirds of the ventricle, but did not expand at the base (Fig. 6 *D*), resulting in an 18% ($P < 0.05$) average increase in the entire ventricle. The increases in left ventricular weight after infarction in nontransgenics (23±3%) and transgenics (15±4%) were then compared, and the 35% smaller increase of this parameter in FVB.Igf+/− (15: 23 = 0.65, i.e., −35%) was statistically significant ($P < 0.001$). Moreover, the 27±5% increase in right ventricular weight in nontransgenics and the 13±4% increase in transgenics with infarction indicated a 52% lesser increase in weight in the latter group of animals (13: 27 = 0.48, i.e., −52%) which was also statistically significant ($P < 0.001$).

After infarction, the longitudinal axis of the left ventricle increased 16% ($P < 0.001$) in nontransgenics, from 7.5±0.34 to 8.7±0.52 mm, and 18% ($P < 0.001$) in FVB.Igf+/−, from 7.7±0.37 to 9.1±0.48 mm. Moreover, chamber volume increased 131% ($P < 0.001$) in nontransgenics, from 65±11 to 149±27 μl, and 68% ($P < 0.005$) in FVB.Igf+/−, from 83±15 to 139±44 μl. The 28% larger chamber volume in control FVB.Igf+/− mice was significant ($P < 0.01$). In contrast, the differential changes in chamber volume after infarction in nontransgenic and transgenic mice resulted in a similar cavitary size in the two groups of mice. When the different reduction in wall thickness after infarction between nontransgenics (−29±6%) and transgenics (−17±5%) was examined on a statistical basis, it was possible to demonstrate that IGF-1 overexpression was associated with a 41% ($P < 0.001$) smaller decrease in this parameter (17: 29 = 0.59, i.e., −41%). Similarly, the 43±9% increase in chamber diameter in nontransgenics and the 18±6% increase in transgenics resulted in a 58% lesser augmentation in cavitary diameter in the latter group (18: 43 = 0.42, i.e., −58%). Finally, the 131±17% expansion in chamber volume in infarcted nontransgenics, and the 68±20% increase in infarcted transgenics yielded a 48% ($P < 0.001$) smaller change in left ventricular chamber volume in transgenics (68: 131 = 0.52, i.e., −48%).

The measurements of wall thickness and chamber diameter were combined with the in vivo evaluations of LVEDP to compute the distribution of diastolic wall stress from base to apex. In infarcted nontransgenics, this parameter increased 348% ($P < 0.001$) at the base, 344% ($P < 0.001$) in the midregion, and 550% ($P < 0.001$) in the apical area (Fig. 7 *A*). Corresponding changes in diastolic wall stress in infarcted transgenics were 149% ($P < 0.001$), 261% ($P < 0.001$), and 353% ($P < 0.001$) (Fig. 7 *B*). As a consequence, diastolic stress from base to apex increased 2.3-fold ($P < 0.005$), 1.3-fold ($P < 0.05$), and 1.6-fold ($P < 0.05$) more in nontransgenic than in FVB.Igf+/− mice. In the entire ventricle, diastolic wall stress was 1.6-fold ($P < 0.005$) higher in infarcted nontransgenics. A similar pattern was noted in the septum. The increases in diastolic septal stress in infarcted nontransgenics varied from a minimum of 255% ($P < 0.001$) to a maximum of 299% ($P < 0.001$), with a mean value of 270% ($P < 0.001$) (Fig. 7 *C*). Lower increases were seen in the septum of infarcted FVB.Igf+/− (Fig. 7 *D*). The average 1.7-fold higher elevation in diastolic septal stress in nontransgenics was significant ($P < 0.01$).

Discussion

IGF-1 and myocyte cell death. This study demonstrates that overexpression of IGF-1 in transgenic mice was capable of interfering with myocyte death in the region adjacent to the infarcted myocardium, attenuating ventricular dilation and the magnitude of the overload. In contrast, cell apoptosis and ne-

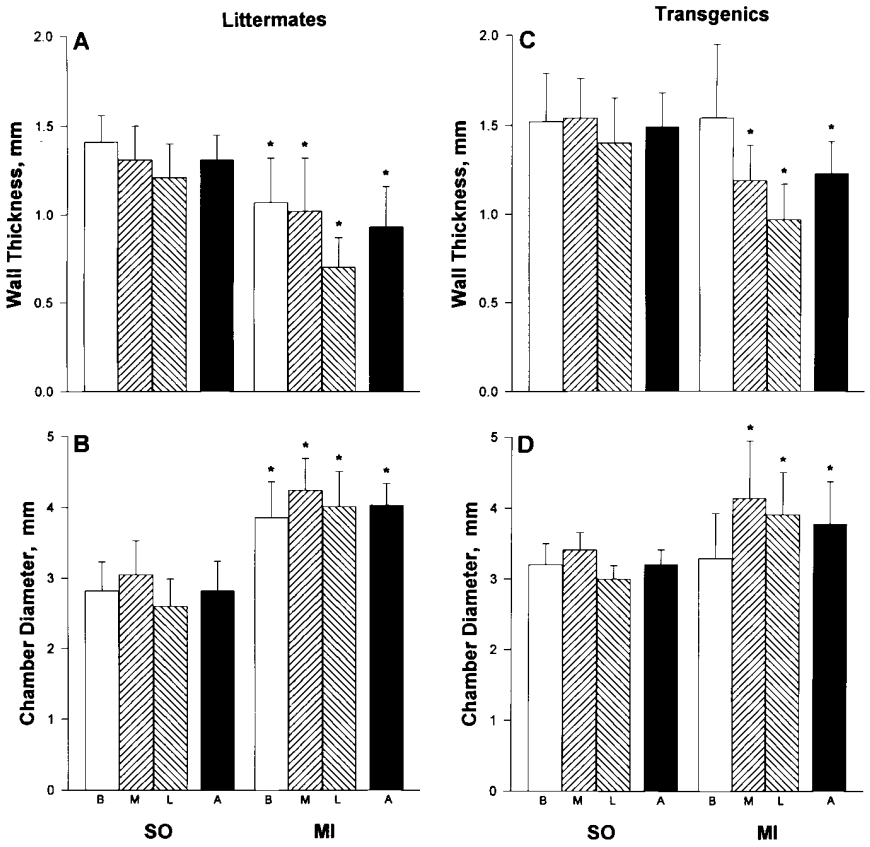

Figure 6. Effects of infarction (*MI*) on left ventricular free wall thickness and chamber diameter at the base (*B*), midregion (*M*), lower apical portion (*L*), and as an average in the entire ventricle (*A*) of nontransgenics and transgenics at 2.5 mo. *Indicates a difference from the corresponding value in SO mice, $P < 0.05$. $n = 10$ in each group.

crosis were enhanced in the surviving myocardium of infarcted nontransgenics. The protective effect against cell death in FVB.Igf+/− mice was independent from ventricular weight and the number and size of myocytes. It was detected in animals at 1.5 mo in which heart weight was not different from nontransgenics, although the number of myocytes was greater and cell volume was smaller (18). A similar behavior was observed in infarcted FVB.Igf+/− at 2.5 mo that had higher heart weight and cell numbers, but myocytes comparable in size to wild-type mice (18). Of relevance, IGF-1 protects in vitro from apoptosis cerebellar neurons (10, 13), hemopoietic cells (9), fibroblasts (11), preovulatory follicles (12), neuroblastoma cells (17), and most importantly, transplanted tumors in vivo (14). Moreover, its administration attenuates myocyte death in ischemia reperfusion injury (15). Results here provide the first demonstration that endogenous overexpression of IGF-1 in myocytes counteracts in vivo the death signal associated with coronary occlusion and a large segmental loss of myocardium. IGF-1, however, was unable to interfere with the magnitude of myocyte death in the portion of the wall supplied by the permanently occluded coronary artery.

The mechanisms by which IGF-1 prevents cell death are unknown. Decreases in the density of IGF-1 receptors (IGF-1R) are characterized by increases in apoptosis (14). A threshold for apoptosis involving a reduction of nearly 50% in IGF-1R has been found, suggesting that the IGF-1–IGF-1R system may regulate the synthesis of apoptosis-inducing molecules (14, 16). These intracellular mediators, however, remain to be identified. IGF-1 overexpression may have the same biological consequence of an upregulation in IGF-1R: inhibiting cell death. IGF-1 may be necessary and sufficient to attenuate cell death, since the expression of IGF-1R in myocytes of FVB.Igf+/− is constant postnatally (unpublished observation from our laboratory). Importantly, IGF-1 may increase the formation and release of nitric oxide from endothelial cells (30) reducing the generation of reactive oxygen species and myocyte apoptosis (8). Additionally, nitric oxide may improve coronary blood supply to the myocardium (30), preventing cell necrosis. IGF-1 also suppresses interleukin-1β-converting enzyme (ICE)–mediated cell death, possibly by inhibiting the cleavage and activation of this enzyme (31). This action of IGF-1 on ICE is independent from the expression of the p53-inducible genes, bax and bcl-2 (31).

IGF-1 and ventricular remodeling. Myocyte death is a common aspect of the pathologic heart (22, 32–36), and animal models mimicking the human disease have provided similar results (7, 20, 37–39). As confirmed here, the extent of scattered apoptotic and/or necrotic myocyte death is small, raising questions on the relevance of a modest chronic loss of myocytes on the progression of the cardiomyopathic heart to ventricular dysfunction and failure (20, 36). The current data, however, demonstrate that a marked increase in ventricular volume occurred in wild mice shortly after infarction, confirming observations in rats (1–6) and humans (1, 40–43). In these cases, myocyte death affected the surviving portion of the myocardium (7, 32, 44) contributing to cavitary dilation (8). Conversely, a nearly 50% smaller increase in chamber volume was seen in FVB.Igf+/− mice in which IGF-1 opposed the impact of infarction on the activation of myocyte death. This finding has no precedent.

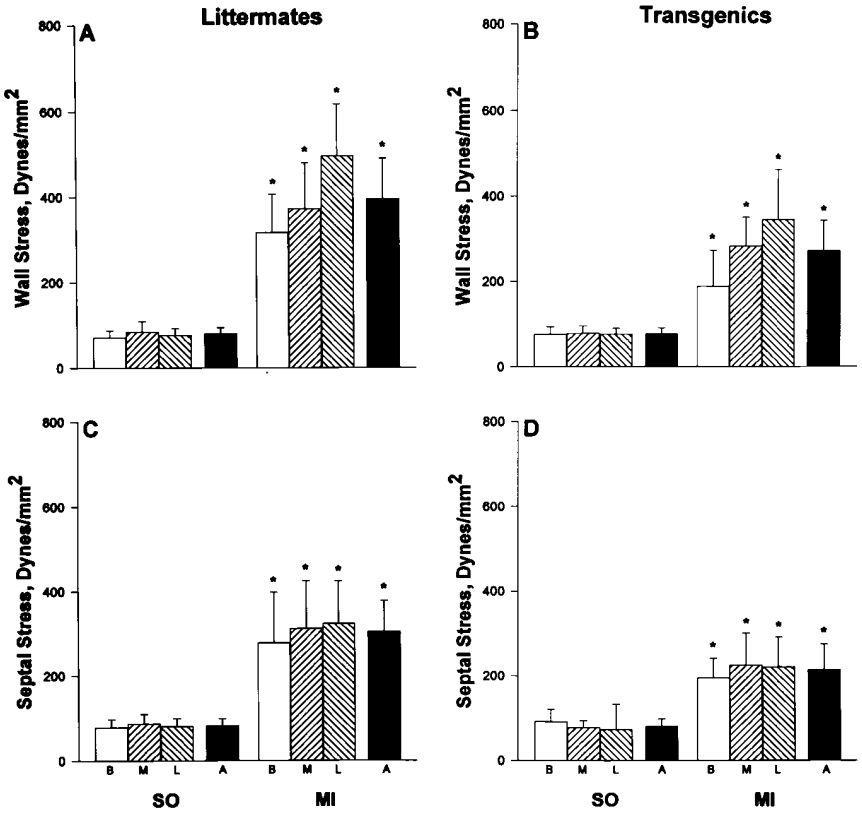

Figure 7. MI on diastolic stress of the left ventricle and septum at the base (*B*), midregion (*M*), lower apical portion (*L*), and as an average in the entire ventricle and septum (*A*) of nontransgenics and transgenics at 2.5 mo. *Indicates a difference from the corresponding value in SO mice, $P < 0.05$. $n = 10$ in each group.

Ventricular dilation is a critical complicating event of myocardial infarction (1, 4, 5, 41–43). The cellular mechanisms implicated in the increase in cavitary volume have been characterized. Muscle fiber slippage is an early negative reaction of the viable region of the wall to the elevated diastolic pressure, and accounts for most of mural thinning and ventricular dilation acutely after infarction (2, 6). This type of wall restructuring requires scattered myocyte death (7, 8, 32, 44). A second mechanism concerns cellular hypertrophy and progressive increases in myocyte length (4, 23, 45); fiber elongation provides a structural template for a larger cavitary volume chronically. Third, myocyte regeneration with in series addition of newly formed cells may contribute to long-term ventricular dilation (46, 47). Finally, thinning of the infarcted region with healing expands chamber volume acutely and subacutely (1–3). The 41% smaller decrease of mural thickness in the absence of cell death in infarcted FVB.Igf+/− suggests that the protective effect of IGF-1 on cell survival most likely interfered with the magnitude of cell slippage in the myocardium. IGF-1 overexpression may have also influenced the degree of myocyte lengthening, insertion of new cells in the wall, and shrinkage of the necrotic tissue.

IGF-1 and wall stress. After large infarcts, there is a significant increase in diastolic wall stress (1, 5, 41, 43). Diastolic Laplace overloading occurs acutely and persists subacutely and chronically in the postinfarcted heart. Diastolic dysfunction is not reversed by hypertrophy of the surviving myocytes that nearly double in volume (23, 45) without ameliorating cardiac performance (6, 45, 48). The increased preload maintains a mechanical stimulus for myocyte lengthening (48–50), expanding chamber diameter and enhancing diastolic stress (5). As shown here, FVB.Igf+/− mice sustained more efficiently the effects of myocardial infarction, since the increases in diastolic wall stress were nearly 40% lower than in nontransgenics. Moreover, the increases in weight of the left and right ventricles were 35 and 52% smaller in FVB.Igf+/− mice than in nontransgenics. These attenuations in pathologic loads and cardiac hypertrophy may positively influence the long-term outcome of the cardiomyopathic heart of ischemic origin.

It should be emphasized that FVB.Igf+/− mice at 2.5 mo of age had hypertrophied hearts and larger chamber volumes. Since infarct size was measured by the fraction of damaged tissue in the ventricle, similar percentages in the two groups of animals reflected in absolute terms greater masses of infarcted myocardium in transgenics. Moreover, cavitary dilation negatively influences the outcome of myocardial infarction (1, 41–43) and potentiates the onset of ventricular dysfunction and failure (51, 52). These phenomena have to be considered when interpreting the accumulated results, which may have underestimated the beneficial action of IGF-1 in these experiments. The protective ability of IGF-1 was observed in spite of the presence of cardiac hypertrophy and a greater cavitary size. Importantly, myocardial hypertrophy is associated with more severe impairment in ventricular hemodynamics and increased morbidity and mortality after infarction (53–55). These major risk factors of the hypertrophied heart are independent from infarct size (54), which represents an additional critical event. The smaller increase in chamber volume in transgenic mice after infarction cannot be attributed to its larger size before coronary occlusion. Postinfarction ventricular dilation is largely the consequence of the elevation in diastolic wall stress that is coupled with scattered myocyte cell death, side-to-side slippage of

myocytes within the wall, mural thinning, and increased cavitary diameter (5, 6). A cause and effect relationship between diastolic Laplace overloading and these structural alterations has been shown in in vitro preparations (8). Abnormal increases in diastolic stress condition not only acute ventricular dilation, but also the progressive increase in cavitary size chronically after infarction (6, 45). This form of remodeling involves the in series insertion of new sarcomeres within the cells as well as myocyte lengthening. Since myocyte cell volume was comparable in control and transgenic mice before coronary artery occlusion (18), the smaller increase in diastolic wall stress in the infarcted FVB.Igf+/− mice may be regarded as the determinant factor of moderate ventricular dilation in this group. Conversely, myocardial infarction on hypertrophied dilated hearts results in greater degrees of adverse cardiac events (56, 57).

There are two relevant points that have to be addressed. Targeted IGF-1 overexpression in myocytes attenuated myocyte cell death, chamber dilation, and diastolic wall stress after infarction. It is difficult, however, to establish with certainty that the reduction in myocyte loss was the only factor responsible for the limitation in ventricular remodeling in transgenic mice. Caution has to be exercised in the interpretation of in vivo studies in which a cause and effect relationship can hardly be claimed. On the other hand, the current observations, in combination with previous in vivo (5–7, 45) and in vitro (8) experimentations, suggest that inhibition of myocyte death by IGF-1 may have played a significant role in the characterization of the anatomical properties of the infarcted heart. Although this growth factor interfered with myocyte death in the surviving myocardium, global cardiac pump function was impaired in a manner similar to that detected in nontransgenic mice. This impairment may have occurred because only very large infarcts were produced. It was beyond the purpose of this study to analyze the impact of infarcts of different sizes on ventricular hemodynamics; this is an important question to be addressed in the future. Diastolic overloading, however, was reduced in transgenic mice, and this beneficial effect may condition long-term cardiac remodeling and survival in the ischemic myopathy.

Acknowledgments

The technical assistance of Maria Feliciano is greatly appreciated.

This work was supported by grants HL-38132, HL-39902, HL-43023, HL-40561, and AG-00378 (R. Baserga) from the National Institutes of Health, and by a Grant-in-Aid from the American Heart Association, no. 950321.

References

1. Pfeffer, M.A., and E. Braunwald. 1990. Ventricular remodeling after myocardial infarction. *Circulation.* 81:1161–1172.

2. Weisman, H.F., D.E. Bush, J.A. Mannisi, M.L. Weisfeldt, and B. Healy. 1988. Cellular mechanisms of myocardial infarct expansion. *Circulation.* 78: 186–201.

3. DeFelice, A., R. Frering, and P. Horan. 1989. Time course of hemodynamic changes in rats with healed severe myocardial infarction. *Am. J. Physiol.* 257:H289–H296.

4. Pfeffer, J.M., M.A. Pfeffer, P.J. Fletcher, and E. Braunwald. 1991. Progressive ventricular remodeling in rat myocardial infarction. *Am. J. Physiol.* 260:H1406–H1414.

5. Anversa, P., G. Olivetti, L.G. Meggs, E.H. Sonnenblick, and J.M. Capasso. 1993. Cardiac anatomy and ventricular loading after myocardial infarction. *Circulation.* 87:VII22–VII27.

6. Olivetti, G., J.M. Capasso, E.H. Sonnenblick, and P. Anversa. 1990. Side-to-side slippage of myocytes participates in ventricular wall remodeling acutely after myocardial infarction in rats. *Circ. Res.* 67:23–34.

7. Cheng, W., J. Kajstura, J.A. Nitahara, B. Li, K. Reiss, Y. Liu, W.A. Clark, S. Krajewski, J.C. Reed, G. Olivetti, and P. Anversa. 1996. Programmed cell death contributes to ventricular remodeling after myocardial infarction in rats. *Exp. Cell Res.* 226:316–327.

8. Cheng, W., B. Li, J. Kajstura, P. Li, M.S. Wolin, E.H. Sonnenblick, T.H. Hintze, G. Olivetti, and P. Anversa. 1995. Stretch-induced programmed myocyte cell death. *J. Clin. Invest.* 96:2247–2259.

9. Rodriguez-Tarduchy, G., M.K. Collins, I. Garcia, and A. Lopez-Rivas. 1992. Insulin-like growth factor-1 inhibits apoptosis in IL-3-dependent hemopoietic cells. *J. Immunol.* 149:535–540.

10. D'Mello, S.R., C. Galli, T. Ciotti, and P. Calissano. 1993. Induction of apoptosis in cerebellar granule neurons by low potassium: inhibition of death by insulin-like growth factor 1 and cAMP. *Proc. Natl. Acad. Sci. USA.* 90: 10989–10993.

11. Harrington, E.A., M.R. Bennett, A. Fanidi, and G.I. Evan. 1994. c-myc-Induced apoptosis in fibroblasts is inhibited by specific cytokines. *EMBO J.* 13: 3286–3295.

12. Chun, S.Y., H. Billig, J.L. Tilly, I. Furuta, A. Tsafriri, and A.J. Hsueh. 1994. Gonadotropin suppression of apoptosis in cultured preovulatory follicles: mediatory role of endogenous insulin-like growth factor 1. *Endocrinology.* 135: 1845–1853.

13. Galli, C., O. Meucci, A. Scorziello, T.M. Werge, P. Calissano, and G. Schettini. 1995. Apoptosis in cerebellar granule cells is blocked by high KCl, forskolin, and IGF-1 through distinct mechanisms of action: The involvement of intracellular calcium and RNA synthesis. *J. Neurosci.* 15:1172–1179.

14. Resnicoff, M., D. Abraham, W. Yutanawiboonchai, H.L. Rotman, J. Kajstura, R. Rubin, P. Zoltick, and R. Baserga. 1995. The insulin-like growth factor 1 receptor protects tumor cells from apoptosis in vivo. *Cancer Res.* 55: 2463–2469.

15. Buerke, M., T. Murohara, C. Skurk, C. Nuss, K. Tomaselli, and A.M. Lefer. 1995. Cardioprotective effect of insulin-like growth factor 1 in myocardial ischemia followed by reperfusion. *Proc. Natl. Acad. Sci. USA.* 92:8031–8035.

16. Resnicoff, M., J.-L. Burgaud, H.L. Rotman, D. Abraham, and R. Baserga. 1995. Correlation between apoptosis, tumorigenesis, and levels of insulin-like growth factor 1 receptors. *Cancer Res.* 55:3739–3741.

17. Matthews, C.C., and E.L. Feldman. 1996. Insulin-like growth factor 1 rescues SH-SY5Y human neuroblastoma cells from hyperosmotic induced programmed cell death. *J. Cell. Physiol.* 166:323–331.

18. Reiss, K., W. Cheng, A. Ferber, J. Kajstura, P. Li, B. Li, G. Olivetti, C.J. Homcy, R. Baserga, and P. Anversa. 1996. Overexpression of insulin-like growth factor-1 in the heart is coupled with myocyte proliferation in transgenic mice. *Proc. Natl. Acad. Sci. USA.* 93:8630–8635.

19. Nolan, A.C., W.A. Clark, T. Karwoski, and R. Zak. 1983. Patterns of cellular injury in myocardial ischemia determined by monoclonal antimyosin. *Proc. Natl. Acad. Sci. USA.* 80:6046–6050.

20. Kajstura, J., W. Cheng, R. Sarangarajan, P. Li, B. Li, J.A. Nitahara, S. Chapnick, K. Reiss, G. Olivetti, and P. Anversa. 1996. Necrotic and apoptotic myocyte cell death in the aging heart of Fischer 344 rats. *Am. J. Physiol.* 217: H1215–H1228.

21. Kajstura, J., W. Cheng, K. Reiss, W.A. Clark, E.H. Sonnenblick, S. Krajewski, J.C. Reed, G. Olivetti, and P. Anversa. 1996. Apoptotic and necrotic myocyte cell death are independent contributing variables of infarct size in rats. *Lab. Invest.* 74:86–107.

22. Olivetti, G., R. Abbi, F. Quaini, J. Kajstura, W. Cheng, J.A. Nitahara, E. Quaini, C. Di Loreto, C.A. Beltrami, S. Krajewski, et al. 1997. Apoptosis in the failing human heart. *N. Engl. J. Med.* 336:1131–1141.

23. Anversa, P., C. Beghi, Y. Kikkawa, and G. Olivetti. 1986. Myocardial infarction in rats: Infarct size, myocyte hypertrophy and capillary growth. *Circ. Res.* 58:26–37.

24. Capasso, J.M., T. Palackal, G. Olivetti, and P. Anversa. 1990. Left ventricular failure induced by long-term hypertension in rats. *Circ. Res.* 66:1400–1412.

25. Dodge, H.T., H. Sandler, W.A. Baxley, and R.R. Hawley. 1966. Usefulness and limitation of radiographic methods for determining left ventricular volume. *Am. J. Cardiol.* 18:10–23.

26. Anversa, P., X. Zhang, P. Li, and J.M. Capasso. 1992. Chronic coronary artery constriction leads to moderate myocyte loss and left ventricular dysfunction and failure in rats. *J. Clin. Invest.* 89:618–629.

27. Wallenstein, S., C.L. Zucker, and J.L. Fleiss. 1980. Some statistical methods useful in circulation research. *Circ. Res.* 47:1–9.

28. Anversa, P., A.V. Loud, F. Giacomelli, and J. Wiener. 1978. Absolute morphometric study of myocardial hypertrophy in experimental hypertension. II. Ultrastructure of myocytes and interstitium. *Lab. Invest.* 38:597–609.

29. Wyllie, A.H., R.G. Morris, A.L. Smith, and D. Dunlop. 1984. Chromatin cleavage in apoptosis: association with condensed chromatin morphology and dependence on macromolecular synthesis. *J. Pathol.* 142:67–77.

30. Zeng, G., and M.J. Quon. 1996. Insulin-stimulated production of nitric oxide is inhibited by wortmannin. Direct measurement in vascular endothelial

cells. *J. Clin. Invest.* 98:894–898.

31. Jung, Y.K., M. Miura, and J. Yuan. 1996. Suppression of interleukin-1 beta converting enzyme-mediated cell death by insulin-like growth factor, *J. Biol. Chem.* 271:5112–5117.

32. Itoh, G., J. Tamura, M. Suzuki, Y. Suzuki, H. Ikeda, M. Koike, M. Nomura, T. Jie, and K. Ito. 1995. DNA fragmentation of human infarcted myocardial cells demonstrated by the nick end labeling method and DNA agarose gel electrophoresis. *Am. J. Pathol.* 146:1235–1331.

33. Bardales, R.H., S. Hailey, S.S. Xie, R.F. Schaefer, and S.-M. Hsu. 1996. In situ apoptosis assay for the detection of early acute myocardial infarction. *Am. J. Pathol.* 149:821–829.

34. Narula, J., N. Haider, R. Virmani, T.G. DiSalvo, F.D. Kolodgie, R.J. Hajjar, U. Schmidt, M.J. Semigran, G.W. Dec, and B.-A. Khaw. 1996. Apoptosis in myocytes in end-stage heart failure. *N. Engl. J. Med.* 335:1182–1189.

35. Mallat, Z., A. Tedgui, F. Fontaliran, R. Frank, M. Durigon, and G. Fontaine. 1996. Evidence of apoptosis in arrhythmogenic right ventricular dysplasia. *N. Engl. J. Med.* 335:1190–1196.

36. Colucci, W.S. 1996. Apoptosis in the heart. *N. Engl. J. Med.* 335:1224–1226.

37. Gottlieb, R.A., K.O. Burleson, R.A. Kloner, B.M. Bablor, and R.L. Engler. 1994. Reperfusion injury induces apoptosis in rabbit cardiomyocytes. *J. Clin. Invest.* 94:1621–1628.

38. Sharov, V.G., H.N. Sabbah, H. Shimoyama, A.V. Goussev, M. Lesch, and S. Goldstein. 1996. Evidence of cardiocyte apoptosis in myocardium of dogs with chronic heart failure. *Am. J. Pathol.* 148:141–149.

39. Li, Z., O.H.L. Bing, X. Long, K.G. Robinson, and E.G. Lakatta. 1997. Increased cardiomyocyte apoptosis during the transition from hypertrophy to heart failure in the spontaneously hypertensive rat. *Am. J. Physiol.* 272:H2313–H2319.

40. McKay, R.G., M.A. Pfeffer, R.C. Pasternak, J.E. Markis, P.C. Come, S. Nakao, J.D. Alderman, J.J. Ferguson, R.D. Safian, and W. Grossman. 1986. Left ventricular remodeling following myocardial infarction: a corollary to infarct expansion. *Circulation.* 74:693–702.

41. Pfeffer, M.A., G.A. Lamas, D.E. Vaughan, A.F. Parisi, and E. Braunwald. 1988. Effects of captopril on progressive ventricular dilation after anterior myocardial infarction. *N. Engl. J. Med.* 319:80–86.

42. Pfeffer, M., E. Braunwald, L. Moye, L. Basta, E.J. Brown, Jr., T.E. Cuddy, B.R. Davis, E.M. Geltman, S. Goldman, G.C. Flaker, et al. 1992. Effect of captopril on mortality and morbidity in patients with left ventricular dysfunction after myocardial infarction: results of the survival and ventricular enlargement trial: the SAVE Investigators. *N. Engl. J. Med.* 327:669–677.

43. Grossman, W., and B.H. Lorell. 1993. Hemodynamic aspects of left ventricular remodeling after myocardial infarction. *Circulation.* 87:VII28–VII30.

44. Olivetti, G., F. Quaini, R. Sala, C. Lagrasta, D. Corradi, E. Bonacina, S.R. Gambert, E. Cigola, and P. Anversa. 1996. Acute myocardial infarction in humans is associated with activation of programmed myocyte cell death in the surviving portion of the heart. *J. Mol. Cell. Cardiol.* 28:2005–2016.

45. Olivetti, G., J.M. Capasso, L.G. Meggs, E.H. Sonnenblick, and P. Anversa. 1991. Cellular basis of chronic ventricular remodeling after myocardial infarction in rats. *Circ. Res.* 68:856–869.

46. Linzbach, A.J. 1960. Heart failure from the point of view of quantitative anatomy. *Am. J. Cardiol.* 5:370–382.

47. Kajstura, J., X. Zhang, K. Reiss, E. Szoke, P. Li, C. Lagrasta, W. Cheng, Z. Darzynkiewicz, G. Olivetti, and P. Anversa. 1994. Myocyte cellular hyperplasia and myocyte cellular hypertrophy contribute to chronic ventricular remodeling in coronary narrowing induced cardiomyopathy in rats. *Circ. Res.* 74: 383–400.

48. Li, P., C. Park, R. Micheletti, B. Li, W. Cheng, E.H. Sonnenblick, P. Anversa, and G. Bianchi. 1995. Myocyte performance during evolution of myocardial infarction in rats: effects of propionyl-L-carnitine. *Am. J. Physiol.* 268: H1702–H1713.

49. Grossman, W., D. Jones, and L.P. McLaurin. 1975. Walls stress and patterns of hypertrophy in the human left ventricle. *J. Clin. Invest.* 56:56–64.

50. Beltrami, C.A., N. Finato, M. Rocco, G.A. Feruglio, C. Puricelli, E. Cigola, F. Quaini, E.H. Sonnenblick, G. Olivetti, and P. Anversa. 1994. Structural basis of end-stage failure in ischemic cardiomyopathy in humans. *Circulation.* 89:151–163.

51. Vasan, R.S., M.G. Larson, E.J. Benjamin, J.C. Evans, and D. Levy. 1997. Left ventricular dilation and the risk of congestive heart failure in people without myocardial infarction. *N. Engl. J. Med.* 336:1350–1355.

52. Poole-Wilson, P.A. 1997. Prediction of heart failure—an art aided by technology. *N. Engl. J. Med.* 336:1381–1382.

53. Mueller, T.M., R.J. Tomanek, R.E. Kerber, and M.L. Marcus. 1980. Myocardial infarction in dogs with chronic hypertension and left ventricular hypertrophy. *Am. J. Physiol.* 239:H731–H735.

54. Koyanagi, S., C.L. Eastham, D.G. Harrison, and M.L. Marcus. 1982. Increased size of myocardial infarction in dogs with chronic hypertension and left ventricular hypertrophy. *Circ. Res.* 50:55–62.

55. Koyanagi, S., C.L. Eastham, and M.L. Marcus. 1982. Effects of chronic hypertension and left ventricular hypertrophy on the incidence of sudden cardiac death after coronary artery occlusion in conscious dogs. *Circulation.* 65: 1192–1197.

56. Galderisi, M., M.S. Lauer, and D. Levy. 1992. Echocardiographic determinants of clinical outcome in subjects with coronary artery disease (the Framingham Heart Study). *Am. J. Cardiol.* 70:971–976.

57. St. John Sutton, M., M.A. Pfeffer, T. Plappert, J.-L. Rouleau, L.A. Moyé, G.R. Dagenais, G.A. Lamas, M. Klein, B. Sussex, S. Goldman, et al. 1994. Quantitative two-dimensional echocardiographic measurements are major predictors of adverse cardiovascular events after acute myocardial infarction. The protective effects of captopril. *Circulation.* 89:68–75.